OPTIMUM DESIGN OF 3R ORTHOGONAL MANIPULATORS CONSIDERING ITS TOPOLOGY

Giovana Trindade da Silva Oliveira, gtrindadeso@yahoo.com.br
School of Mechanical Engineering, Federal University of Uberlândia, 2160 João Naves de Ávila Av., Campus Santa Mônica, CEP 38400-902, Uberlândia, Brazil.

Antônio Carlos Nogueira, anogueira@ufu.br
Sezimária Fátima Pereira Saramago, saramago@ufu.br
College of Mathematics, Federal University of Uberlândia, 2160 João Naves de Ávila Av., Campus Santa Mônica, CEP 38400-902, Uberlândia, Brazil.

Abstract. *Several studies have investigated the properties of the workspace of robotic chains opened with the purpose of emphasizing its geometric and kinematic characteristics, to devise analytical algorithms and procedures for its design. The workspace of a manipulator robot is considered of great interest from theoretical and practical viewpoint. In this paper, the workspace topology is defined by the number of kinematic solutions, the number of cusps and nodes that appear on the workspace boundary. In the classical cases used in Industry, manipulators, to change posture, need to pass through a singularity of the joint space. A 3-revolute (3R) manipulator can execute a non singular change of posture if and only if there is at least one point in its workspace with exactly three coincident inverse kinematic solutions. In this work, a mulit-objective optimization problem is formulated with the aim of obtaining the optimal geometric parameters of robot which must obey the topology specified by the designer. The maximum workspace volume, the maximum system stiffness and the optimum dexterity are considered as multi-objective functions. In addition, the optimization problem is subject to penalties that control the topology, forcing it to occupy a certain portion of the workspace. One sequential technique and two evolution algorithms are applied to obtain the problem solution. Two applications are presented to show the efficiency of the proposed methodology.*

Keywords*: robotics, manipulators topology, optimization, workspace volume, robot stiffness, robot dexterity.*

1. INTRODUCTION

In the classical cases used in Industry, manipulators, to change posture, need to pass through a singularity of the joint space. In other words, the end effector must bump into the frontier of the workspace. But this behavior is not general at all.

A manipulator with three rotational joints (3R) can execute a non singular change of posture if and only if there is at least one point in its workspace which has exactly three coincident solutions of the inverse kinematic model (IKM), resulting in one of the separation surfaces which divide the workspace in several regions, called of domains, with manipulators which have same properties (binary or quaternary, regions with the same number of cusp points and nodes). So, to study such manipulators is essential to know the topology of the singularity surfaces in the workspace. These singularities are defined as places where the determinant of the Jacobian matrix of direct kinematic model (DKM) is annulled, defining the equations others of surfaces which divide the workspace.

Wenger and El Omri (1996) showed that for some choices of the parameters, 3R manipulators may be able to change posture without meeting a singularity in the joint space. They succeeded in characterizing such manipulators but they needed general conditions on the design parameters. Corvez and Rouillier (2002) found important results about this issue. In 2004, Baili presented a formulation of the surfaces that separate the different types of 3R manipulators with orthogonal axes and made a classification in the parameters space.

As an application of the classification of the parameters space, Oliveira *et al.* (2008) presented formulated optimization problems with aim of obtaining the optimal geometric parameters of orthogonal 3R manipulators so as to maximize the workspace for topologies pre-determined.

In this paper, the multi-objective optimization problem is formulated with aim of obtaining the optimal geometric parameters of orthogonal 3R manipulators which maximize the workspace volume and the system stiffness and optimizes the dexterity. Moreover, the topology constraints specified by the designer must be obeyed.

This paper also makes a comparative study of three numerical techniques, i.e., sequential quadratic programming (SQP), genetic algorithms (GA) and differential evolution (DE).

The presence of voids, singularities and generation of the discontinuous envelopes can to increase the complexity of the algebraic formulation for a correct mathematical model of the robot. Moreover, the objective function can to present several local maxima and be nonlinear. These factors increase the difficulties involved in the optimization process, justifying the use of different optimization techniques to validate the results.

It is known that conventional methods are based on rule of point-to-point and they have the danger of "falling" into local optima, while the evolutionary algorithms are based on rule of population-to-population.

Evolutionary algorithms have advantages of robustness and properties good of convergence. They not require knowledge on the function gradient or informations about the optimization problems, in this case only the objective function and corresponding fitness levels can influence the directions of search. They use probabilistic transition rules and they solve well the large-scale optimization problems in the presence of local optimal, discontinuities and nonlinearities.

Genetic algorithms and differential evolution have been shown efficient to solve linear and nonlinear problems by exploring all regions of search space and exploiting promising areas through operators of mutation, crossover and selection applied to individuals in the population. Therefore, they are suitable for the optimization problems studied here.

The Fig. 1 illustrates manipulators with three rotational joints and orthogonal axes. The study of this type of manipulator is done according to the Denavit-Hartenberg parameters: d_2, d_3, d_4, r_2, and r_3. To reduce the number of parameters, will be considered $d_2 = 1$ and $r_3 = 0$. The joint variables, which represent the input angles of the actuators, are θ_1, θ_2 and θ_3. For this type of manipulator, the direct kinematic model is given in Eq. (1):

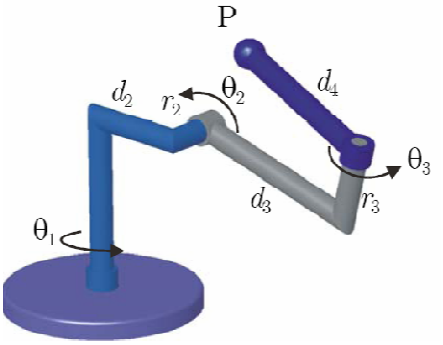

Figure 1. 3R Manipulator with orthogonal axes

$$x = \left[1 + \left(d_3 + d_4 c_3\right) c_2\right] c_1 - \left(r_2 + d_4 s_3\right) s_1$$

$$y = \left[1 + \left(d_3 + d_4 c_3\right) c_2\right] s_1 + \left(r_2 + d_4 s_3\right) c_1 \qquad (1)$$

$$z = -\left(d_3 + d_4 c_3\right) s_2$$

in which $c_i = \cos\theta_i$ and $s_i = \sin\theta_i$, for $i = 1, 2, 3$.

By using the powerful algebraic tool Grobner basis, it is possible to obtain analytical expressions of the surfaces of the parameters space that separate the different types of manipulators. The annulment of the determinant of Jacobian matrix of the inverse kinematic model (IKM) enables to obtain the others surfaces that separate the various regions of topologies (Corvez and Rouillier, 2002; Baili, 2004; Oliveira *et al.*, 2009). Thus, it is possible obtain:

$$C_1 : d_4 = \sqrt{\frac{1}{2}\left(d_3^2 + r_2^2 - \frac{\left(d_3^2 + r_2^2\right)^2 - d_3^2 + r_2^2}{AB}\right)}, \text{ where } A = \sqrt{(d_3+1)^2 + r_2^2} \text{ and } B = \sqrt{(d_3-1)^2 + r_2^2} \qquad (2)$$

The Equation (2) is the surface of separation between the manipulators of domain 1 and domain 2. The manipulators that belong to domain 1 are binary, have a toroidal cavity in its workspace and do not have cusps and nodes points. The domain 2 represents the manipulators that have 4 points of cusp, but do not have the same number of nodes.

The surface of separation C_2, between the domains 2 and 3, is defined by:

$$C_2 : d_4 = d_3 / (1 + d_3).\sqrt{\left(d_3 + 1\right)^2 + r_2^2} \qquad (3)$$

The domain 3 is composed by manipulators which present 2 cusps points on internal envelopment. In the case of domain 4, the manipulators have 4 points of cusp and 4 nodes. The surface C_3, which separates the manipulators of the domains 3 and 4, is given by:

$$C_3 : d_4 = d_3 / (d_3 - 1).\sqrt{\left(d_3 - 1\right)^2 + r_2^2}, \text{ with } d_3 > 1 \qquad (4)$$

Finally, the domain 5 corresponds to manipulators that have no cusp points. Unlike of manipulators of the type 1, the internal envelope is not defined by a toroidal cavity, but by a region with 4 solutions in IKM. The surface of separation C_4, between the domains 3 and 5, is:

$$C_4 : d_4 = d_3 / (1 - d_3).\sqrt{\left(d_3 - 1\right)^2 + r_2^2}, \text{ with } d_3 < 1 \qquad (5)$$

Summarizing, the space of parameters (d_3, d_4 and r_2) of a 3R orthogonal manipulator is divided into 5 domains separated by surfaces C_1, C_2, C_3 and C_4, defined by Eqs. (2), (3), (4) and (5), respectively.

The Figure 2a) shows the curves of separation in a plane section (d_3, d_4) of the space of parameters, resulting in 5 domains, adopting a fixed value for r_2 =1. The Figure 2b) shows the space of parameters divided according to the number of cusps points and nodes points. The domains according to the number of cusps points are divided into sub-domains that contain the same number of nodes. Each sub-domain defines a topology of the workspace denoted $WT_i(\alpha, \beta)$, where α represents the number of cusp points and β the number of nodes points.

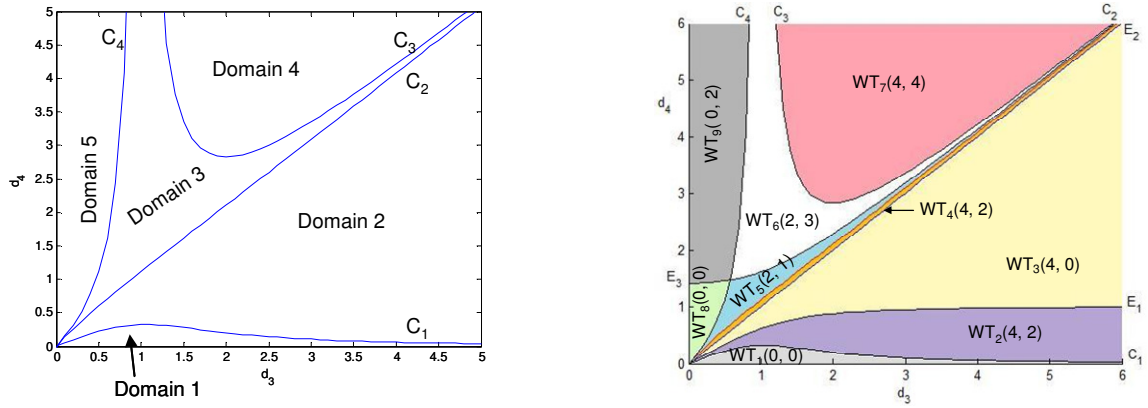

(a) (b)

Figure 2. Division of parameters space considering r_2 = 1:
(a) According to the surface of separation of topologies; (b) According to the number of points of cusps and nodes

As explained previously, the manipulators of the domain 1 have a toroidal cavity and do not have cusps and nodes points. The manipulator represented in Fig. 3a) characterize the first type of manipulator, whose topology is known as $WT_1(0, 0)$.

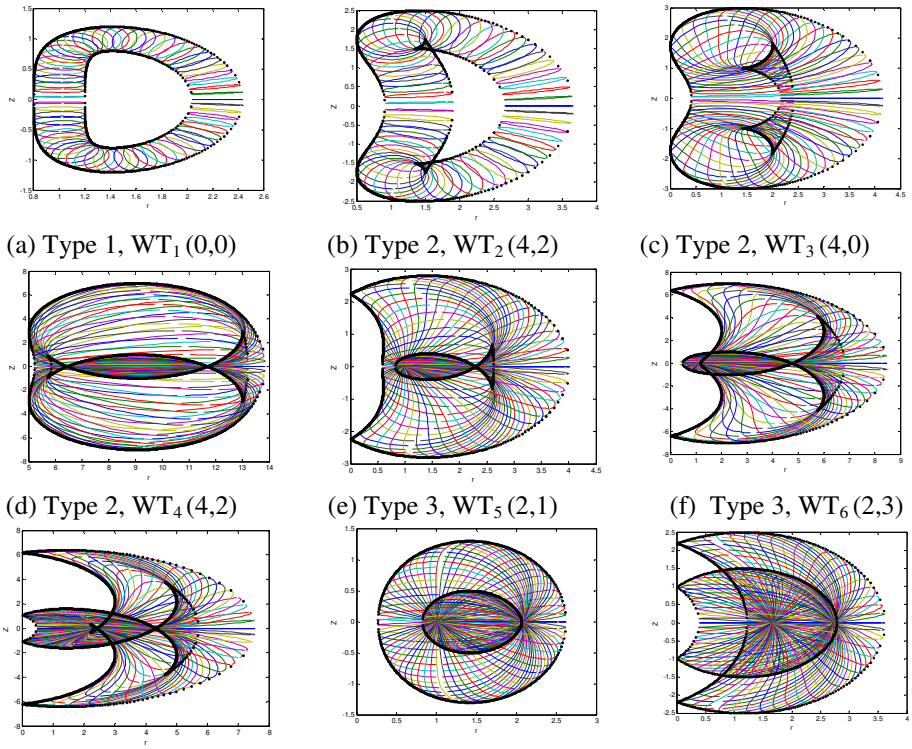

(a) Type 1, WT_1 (0,0) (b) Type 2, WT_2 (4,2) (c) Type 2, WT_3 (4,0)

(d) Type 2, WT_4 (4,2) (e) Type 3, WT_5 (2,1) (f) Type 3, WT_6 (2,3)

(g) Type 4, WT_7 (4,4) (h) Type 5, WT_8 (0,0) (i) Type 5, WT_9 (0,2)

Figure 3. Radial section for 3R orthogonal manipulators, showing the 5 types of manipulators

The manipulators that belong to domain 2 have 4 points of cusp. This region can be subdivided into 3 sub-domains through the surfaces E_1 and E_2. The topology of the workspace $WT_2(4, 2)$, represented by Fig. 3b), has 4 cusp points, 2 nodes, a toroidal cavity, two regions with 4 solutions and a region with 2 solutions in IKM. The topology $WT_3(4, 0)$ contains manipulators with 4 cusp points, zero node, without toroidal cavity, a region with 4 solutions and other with 2 solutions in IKM, as illustrated in Fig. 3c). The transition between the topologies WT_2 and WT_3 is the boundary

between the manipulators containing a toroidal cavity in its workspace and those that do not contain. According to Baili (2004), the surface of separation between these topologies is given by the expression:

$E_1 : d_4 = 0.5\ (A - B)$, where A and B are given in Eq. (2). (6)

In domain 2 is still possible to characterize the topology represented in the Fig. 4d), denoted by $WT_4(4, 2)$, containing 4 points of cusp and 2 nodes. These nodes are different from nodes of WT_2 since not delimit a toroidal cavity but a region of 4 solutions in IKM. In this case, the surface of separation E_2, between topology WT_3 and WT_4 is defined by:

$E_2 : d_4 = d_3$ (7)

The domain 3 is composed by manipulators which have 2 cusp points and can be divided into 2 sub-domains through the surface E_3. The manipulators described by $WT_5(2, 1)$ have 2 cusps points on internal envelope, a node point and has the shape of a fish, as shown the radial section presented in Fig. 3e). Moreover, the Fig. 5f) presents a radial section of a manipulator that belongs to the topology $WT_6(2, 3)$, it has 2 points of cusp and 3 nodes. The Eq. (8) defines the separation surface between the topology WT_5 and WT_6. Besides, this surface also separates the topology of the workspace WT_8 and WT_9 that are contained in the domain 5.

$E_3 : d_4 = 0.5\ (A + B)$ (8)

In domain 4, the manipulators are of type 4, represented by $WT_7(4, 4)$, have 4 cusp points and 4 nodes, as can be seen in Fig. 3g). The 4 points of cusp are shared between the internal and external singularity surfaces.

Finally, the domain 5 corresponds to manipulators that have no cusp points. Unlike of manipulators of the type 1, the internal envelopment is not defined by a toroidal cavity, but by a region with 4 solutions in IKM.

The domain 5 corresponds to manipulators of type 5 and do not have cusp points. This region is divided into 2 sub-domains through the surface E_3. In the Fig. 3h), the topology represented by $WT_8\ (0, 0)$ does not have cusp points and nor nodes. As mentioned earlier, its internal envelope is not defined by a toroidal cavity, but by a region with 4 solutions in IKM. Finally, Fig. 3i) features a manipulator which belongs to the topology $WT_9\ (0, 2)$, with 0 cusp points and 2 nodes points obtained by the intersection of internal and external envelopment.

2. WORKSPACE OF 3R MANIPULATORS

According to Bergamaschi *et al.* (2006), the workspace W is the set of all attainable points for a point P of the end-effector when the joint variables sweep its definition interval entire. Point P is usually chosen as the center of the end-effector, or the tip of a finger, or even the end of the manipulator itself. The first procedure to investigate the workspace is to vary the angles θ_1, θ_2 and θ_3 in their interval of definition and to estimate the coordinates of point P with respect to the manipulator base frame. The workspace of this robot is a solid of revolution. Thus, it is natural to imagine that the workspace is the result of rotation around the z axis of a radial plane section.

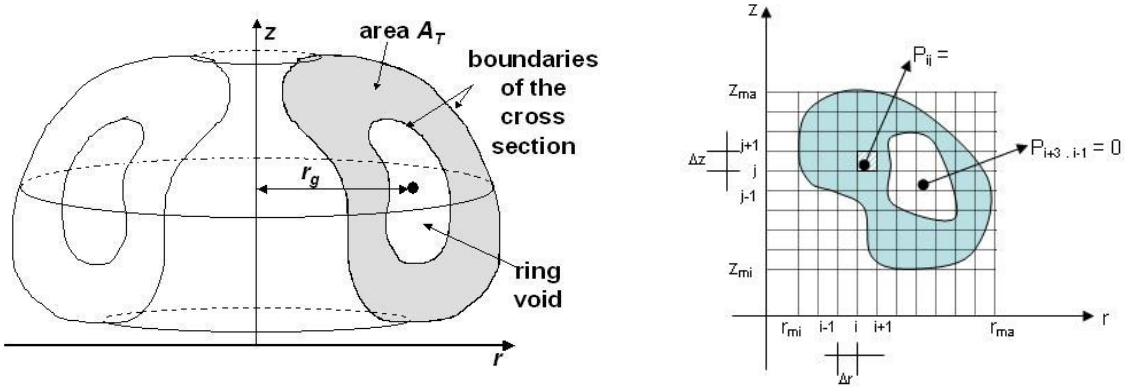

Figure 4. (a) A scheme for evaluating the workspace volume of 3R manipulators; (b) Discretization of radial section area by using a rectangular mesh

The workspace of a three-revolute open chain manipulator can be given in the form of the radial reach r and axial reach z with respect to the base frame, according to Bergamaschi *et al.* (2006). For this representation, r is the radial distance of a generic workspace point from the z-axis, and z is the distance of this same point at the XY-plane (see, Fig. 4b). Thus, using Eq. (1), the parametric equations (of parameters θ_2 and θ_3) of the geometrical locus described by point

P on a radial plane are:

$r^2 = x^2 + y^2$ and z, where x, y and z are given in (1). (9)

The workspace volume *V* can be evaluated by the Pappus-Guldin Theorem, using the following equation (see Fig. 4a):

$V = 2\pi r_g A_r$, where A_r is the cross section area, which is formed by the family of curves given by Eq. (1). (10)

This research proposes numerical formulation to approximate the cross section area, through its discretization within a rectangular mesh. Initially, the extreme values of vectors *r* and *z* should be obtained as:

$r_{min} = \min\{r\}, \quad r_{max} = \max\{r\}, \quad z_{min} = \min\{z\}$ and $z_{max} = \max\{z\}$ (11)

Adopting n_r and n_z as the number of intervals chosen for the discretization along the *r* and *z* axis, the sizes of the elementary areas of the mesh can be calculated:

$$\Delta r = (r_{\max} - r_{\min})/n_r \quad \text{and} \quad \Delta z = (z_{\max} - z_{\min})/n_z \tag{12}$$

The n_r and n_z values must be adopted so that the sizes of the elementary areas (Δr or Δz) are at least 1% of the total distances considered in the discretization (r_{max} - r_{min} or z_{max} - z_{min}). Every point of the family of curves form the cross section of the workspace is calculated by Eq. (9). Using this equation, varying the values of θ_2 and θ_3 in the interval [$-\pi$, π], it is possible to obtain the family of curves of the workspace. Given a certain point (r, z), its position inside the discretization mesh is determined through the following index control:

$$i = \text{int}[(r - r_{\min})/\Delta r] + 1 \quad \text{and} \quad j = \text{int}[(z - z_{\min})/\Delta z] + 1, \tag{13}$$

where *i* and *j* are computed as integer numbers. As shown in Fig. 4b), the point of the mesh that belongs to the workspace is identified by $P_{ij} = 1$, otherwise $P_{ij} = 0$, which means:

$P_{ij} = 0$, if $P_{ij} \notin W(P)$ *or* 1, *if* $P_{ij} \in W(P)$; where $W(P)$ indicates workspace region. (14)

In this way, the total area is obtained by the sum of every elementary areas of the mesh that are totally or partially contained in the cross section. In Eq. (14), it is observed that only the points that belong to the workspace contribute to the calculation of the area A_T. The coordinate r_g of the center of the mass is calculated considering the sum of the center of the mass of each elementary area, divided by the total area, using the following equation:

$$A_T = \sum_{i=1}^{i_{\max}} \sum_{j=1}^{j_{\max}} \left(P_{ij}\, \Delta r\, \Delta z \right) \quad \text{and} \quad r_g = \frac{\left(\sum_{i=1}^{i_{\max}} \sum_{j=1}^{j_{\max}} \left(P_{ij}\, \Delta r\, \Delta z \right) \left((i-1)\, \Delta r + (\Delta r/2) + r_{\min} \right) \right)}{A_T} \tag{15}$$

Finally, after the calculation of the cross section area and the coordinate of the center of the mass, given by Eqs. (14) and (15), respectively, the workspace volume of the manipulator can be evaluated by using Eq. (10).

3. SYSTEM STIFFNESS

From the viewpoint of mechanics, the stiffness is the measurement of the ability of a body or structure to resist deformation due to the action of external forces. The stiffness of a serial mechanism at a given point of its workspace can be characterized by its stiffness matrix. This matrix relates the forces and torques applied at the gripper link in Cartesian space to the corresponding linear and angular Cartesian displacements (Rivin, 1999).

Two main methods have been used to establish mechanism stiffness models, namely: matrix analysis of structures, that deals with structures as a combination of elements and nodes (Deblaise *et al.,* 2006; Gonçalves, 2009) and the methods based on the calculation of the serial mechanism's Jacobian matrix (El-Khasawneh and Ferreira, 1999; Company *et al*., 2005) which is adopted in this work.

The matrix *J* is usually termed Jacobian matrix and it is described in Eq. (16), according to Khalil and Dombre, 1999. For the 3R manipulator with orthogonal axes in study, its determinant is given by Eq. (17).

$$[J]=\begin{pmatrix} -\sin\theta_3\cos\theta_2 d_4-\cos\theta_2 r_2 & 0 & -\sin\theta_3 d_4 \\ \sin\theta_3\sin\theta_2 d_4+\sin\theta_2 r_2 & d_3+\cos\theta_3 d_4 & 0 \\ \cos\theta_2 d_3+\cos\theta_2\cos\theta_3 d_4+d_2 & 0 & \cos\theta_3 d_4 \end{pmatrix} \tag{16}$$

$$\det(J)=d_4\left(d_3+d_4\cos\theta_3\right)\left[d_2\sin\theta_3+\left(d_3\sin\theta_3+\left(d_3\sin\theta_3-r_2\cos\theta_3\right)\cos\theta_2\right)\right] \tag{17}$$

The stiffness matrix of the mechanism in the Cartesian space is then given by the Eq. (18), where K_j is the joint stiffness matrix of the mechanism, with K_j=[k_1, k_2, k_3]. In this case, each actuator of the mechanism is modeled as an elastic component. k_i is a scalar representing the joint stiffness of each actuator, being modeled as linear spring:

$$K_C=[J]^T K_j[J] \tag{18}$$

Particularly, in the case where the actuators have the same stiffness, i.e., k=k_1=k_2=k_3, then Eq. (18) will be reduced to:

$$K_C=k[J]^T[J] \tag{19}$$

Furthermore, the diagonal elements of the stiffness matrix are used as the system stiffness values. These elements represent the pure stiffness in each direction, and they reflect the rigidity of machine tools more clearly and directly. The objective function for system stiffness optimization can be written as Eq. (20). In this case, the stiffness index S must be maximized:

$$S=K_{11}+K_{22}+K_{33} \tag{20}$$

4. DEXTERITY

The performance index of a robotic mechanical system is a scalar quantity that measures how good the system behaves regarding the transmission of motion and strength. This index can be defined for all types of robotic mechanical systems, particularly, serial manipulators.

There are several performance indices defined in the literature, this paper uses the condition number *Cond*(*J*) of the Jacobian matrix to measure the dexterity of the 3R manipulators (Angeles, 2003). The index *Cond*(*J*) is defined as the ratio of the largest singular value λ_{max} of J to the smallest one, λ_{min}, i.e.,

$$Cond(J)=|\lambda_{\max}(J)/\lambda_{\min}(J)| \tag{21}$$

Note that *Cond*(*J*) can attain values from 1 to infinity. The condition number attains its minimum value of unity for matrices with identical singular values; such matrices are, thus, called isotropic. On the other side, singular matrices have a smallest singular value that vanishes, and hence, their condition number is infinity. The condition number of J can be thought of as indicating the distortion in the space of joint variables. The larger this distortion, the greater the *Cond*(*J*). Therefore, for optimization of the dexterity, the condition number must to be minimized.

5. NUMERICAL SIMULATIONS

The optimization problem is formulated with the objective of obtaining the optimal geometric parameters of the 3R manipulator to maximize the workspace and the system stiffness and to optimize the dexterity such as the topologies specified by the designer are obeyed. Since the problem have several objectives, it deals with a multi-objective optimization problem, and it is required to find all possible tradeoffs among multiple objective functions that are usually conflicting with each other. The constraints depend on the topology chosen for the robot, according to Fig. 3. In this work, the optimization is investigated using a Sequential Quadratic Programming (SQP), the Differential Evolution (DE) and Genetic Algorithms (AG).

The evolutionary algorithms were developed for unconstrained problems. So, in the case of constrained optimization problems, it is necessary to introduce modifications in this method. This work uses the concept of Penalty Function (Nocedal and Wright, 2000). In this technique, the problems with constrains are transformed in unconstrained problems adding a penalty function $P(x)$ to the original objective function to limit constraint violations. This new objective function is penalized, according to a factor r_p, every time that meets an active constraint. The scalar r_p is a multiplier that quantifies the magnitude of the penalty. For the efficiency of the evolutionary method, a large value of the penalty factor r_p should be used to ensure near satisfaction of all constraints, in this paper, was adopted r_p=1000. Then, the problem can be rewrite as follows:

Maximize $F(x) = f(x) + r_p P(x)$, where $f(x) = [V, Cond(J), S]$ and $P(x) = \max(0, g_j(x))^2$ (22)

Subject to: $g_j(x) \leq 0; j=1,..,k$ and $x^l \leq x_i \leq x^u$, $i=1, 2, 3$

The geometric parameters are the design variables given by $x = (d_3, d_4, r_2)^T$. The lower and upper bounds adopted for the arm length (side constraints) are: $0.1 \leq x_i \leq 3.0$, $i = 1,2,3$.

In this simulation, two methods of multi-objective optimization are utilized: Weighting Objectives Method and Global Criterion Method (L_{2r}-metric and L_{3r}-metric) presented on Oliveira and Saramago (2010).

The weighted sum strategy converts the multi-objective problem vector $f(x)$ into a scalar optimization problem by building a weighted sum of all the objectives as Eq. (23). The weighting coefficients w_i represent the relative importance of each criterion. Thus,

$$\text{Maximize } F(x) = w_1 Vc_1 - w_2 Cond(J) c_2 + w_3 Sc_3 - r_p P(x) \text{ , where } \sum_{i=1}^{3} w_i = 1 \quad (23)$$

where the workspace volume V is given by Eq. (10), the stiffness S is calculated using the Eq. (20) and the condition number $Cond(J)$ is represented in the Eq. (21).

Objective weighting is obviously the most usual substitute model for vector optimization problems. The trouble here is attaching weighting coefficients to each of the objectives. The weighting coefficients do not necessarily correspond directly to the relative importance of the objectives or allow trade-offs between the objectives to be expressed. For the numerical methods for seeking the optimum of (23) so that w_i can reflect closely the importance of objectives, all the functions should be expressed in units of approximately the same numerical values. The best results are usually obtained if $c_i = 1/f_i^o$, where f_i^o represents the ideal solution, that indicates the minimum value of each i-th function. To determine this solution, one must find the minimum attainable for all the objective functions separately. In this case, the vector $f^o = [V_{id}, S_{id}, Cond(J)_{id}]^T$ is ideal for a multi-objective optimization problem.

In Global Criterion Method, the multi-objective optimization problem is transformed into a scalar optimization problem by using a global criterion. The function that describes this global criterion must be defined such as a possible solution close to the ideal solution is found. In this case, the L_{2r}-metric and L_{3r}-metric, are given respectively by:

$$\text{Minimize } F(x) = \left(\left(\frac{V_{id} - V}{V_{id}} \right)^2 + \left(\frac{Cond(J)_{id} - Cond(J)}{Cond(J)_{id}} \right)^2 + \left(\frac{S_{id} - S}{S_{id}} \right)^2 \right)^{1/2} + r_p P(x) \quad (24)$$

$$\text{Minimize } F(x) = \left(\left| \frac{V_{id} - V}{V_{id}} \right|^3 + \left| \frac{Cond(J)_{id} - Cond(J)}{Cond(J)_{id}} \right|^3 + \left| \frac{S_{id} - S}{S_{id}} \right|^3 \right)^{1/3} + r_p P(x) \quad (25)$$

The computational code of the DE was developed in MATLAB® by the authors. The parameters used were: number of population individuals $Np = 15$; 100 generations, representation of individuals by real vectors using multiplier of the difference vector $F = 0.8$ and crossover probability $CR = 0.5$.

The Genetic Algorithms Optimization Toolbox (GAOT) program developed by Houck *et al.* (1985) has been used to perform the GA, adopting $Np = 80$ individuals, 100 generations, crossover and mutation probabilities: 0.60 and 0.02.

The Sequential Quadratic Programming (SQP) it was performed by using the toolbox *fmincon* of the MATLAB®.

5.1 Example 1 - $WT_1(0, 0)$

In this example, is considered an application where the manipulator must belong to the topology WT_1 (see Fig. 2b). In this case, the following constraints must be obeyed:

Side limits: $0.1 < d_3 < 3.0$; $0.1 < d_4 < 3.0$ e $0.1 < r_2 < 3.0$ [u.l.] and (26)
Points below the curve C_1, given by Eq. (2).

The ideal solutions calculated using DE were: V_{id}=315.2980 [u.v.]; $Cond(J)_{id}$=1.1822 S_{id}=35.5516 [u.s.].

It is worth noting that when SQP is applied the optimum depends on the initial estimate provided by the user. Thus, tests were performed for different initial values resulting in different answers. This behavior clearly indicates the presence of several local minima. Several starting points were tested: the upper and lower limits of the search space, the midpoint of the range and the optimal solution obtained by DE. In the results presented in the tables from 1 to 4 the starting points were the solutions obtained by DE.

The optimal results obtained through the optimization procedure Weighting Objectives Method, Eq. (23), are showed in Tab. 1. Observing this table one can be noted that the best solution depends on interest of the designer because each objective function is conflicting with other. In this example, when was adopted the weighting coefficients

equal to 0.8 for the volume (w_1) or for the stiffness (w_3) it was obtained similar results. This is due to the fact that both are maximized and presented a similar behavior. But giving the weighting coefficient equal to 0.8 for the condition number (w_2) it is observed that was obtained a different result and the dexterity was significantly improved. The results indicate that this problem is sensitive to the dexterity value. When this function is prioritized, the optimal volume and stiffness are strongly modified.

Table 1. Optimal results obtained with the Weighting Objectives Method for Example 1.

weighting coefficients w_i	Technique	d_3	d_4 (u.l.)	r_2	Volume (u.v.)	Cond(J)	Stiffness (u.s)	Time (min)
w_1=0.33	DE	0.97	0.73	0.10	58.63	1.87	10.72	67.34
w_2=0.33	GA	0.65	0.44	0.52	25.46	1.19	6.05	117.7
w_3=0.33	SQP	0.64	0.44	0.52	25.32	1.19	6.03	4.92
w_1=0.80	DE	0.96	0.75	0.10	59.59	1.91	10.85	49.22
w_2=0.10	GA	1.01	0.44	0.62	42.88	1.54	8.72	87.54
w_3=0.10	SQP	0.97	0.73	0.10	58.64	1.87	10.72	1.75
w_1=0.10	DE	0.60	0.43	0.48	22.68	1.18	5.63	60.88
w_2=0.80	GA	0.60	0.43	0.49	22.64	1.18	5.63	89.12
w_3=0.10	SQP	0.60	0.40	0.47	22.66	1.18	5.62	1.94
w_1=0.10	DE	0.97	0.74	0.10	59.14	1.89	10.79	56.39
w_2=0.10	GA	1.00	0.44	0.61	42.57	1.51	8.65	121.9
w_3=0.80	SQP	0.97	0.74	0.10	59.01	1.88	10.78	1.14

Table 2. Optimal results obtained with the Global Criterion Method for Example 1.

	Technique	D_3	d_4 (u.l.)	r_2	Volume (u.v.)	Cond(J)	Stiffness (u.s)	Time (min)
L_{2r}-metric	DE	0.95	0.45	0.59	40.87	1.42	8.35	65.17
	GA	0.97	0.45	0.59	41.73	1.45	8.46	87.39
	SQP	0.95	0.45	0.59	40.85	1.42	8.34	3.41
L_{3r}-metric	DE	0.97	0.73	0.10	58.64	1.87	10.72	41.52
	GA	0.92	0.54	0.41	44.33	1.67	8.66	75.45
	SQP	0.94	0.71	0.16	55.95	1.78	10.31	1.22

Table 2 shows the results obtained by using the Global Criterion Method, given in Eqs. (24) and (25). In this technique the idea is to minimize the relative error of functions in relation to ideal values. The solutions obtained represent a compromise between the three objective functions.

Observing the Tab. 1 and Tab. 2 one can check that the sequential and random techniques obtained similar values, differing only in the computational cost. In the case of SQP, the results were good because the initial estimate was the optimal obtained by DE. Using sequential programming, the computational cost was significantly small, but this technique has some limitations, for example: if the model is multimodal, it can "get stuck" in some local solutions; it only handles real variables; the objective function and the constraints must be continuous.

Considering the L_{2r}-metric, the optimal point obtained by Differential Evolution is marked in Fig. 5a). The optimal radial section area of the workspace is presented in Fig. 5b). Comparing the radial section of Fig. 5b) to Fig. 3a), one can observe that the parameters of project result in a manipulator with a bigger volume (the void of the workspace was reduced). The optimal manipulator belonging to the topology WT_1 ($d_2 = 1$, $r_3 = 0$) is represented in Fig. 5c).

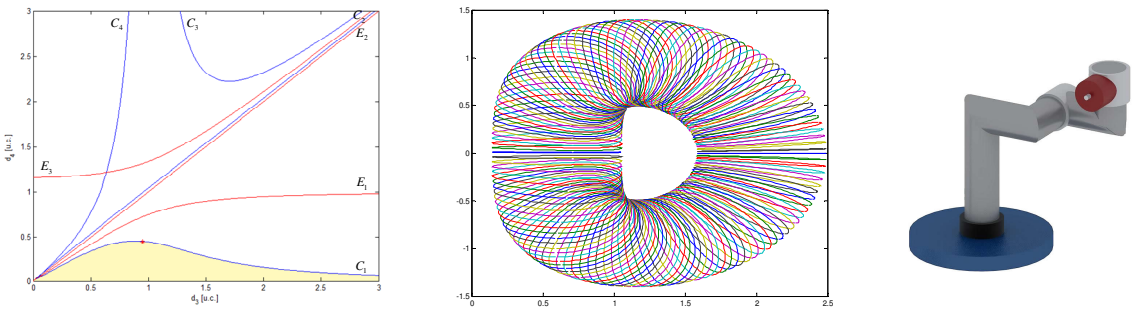

(a) Parameters space with $d_2 = 1$, $r_3 = 0$ (b) Radial section area of the workspace (c) Scheme for 3R Robot

Figure 5. The optimum design of a 3R Robot, considering the L_{2r}-metric by Differential Evolution – Example 1

5.2 Example 2 – WT_3(4, 0)

Now, considering a manipulator that belongs to the topology WT_3, the following constraints are adopted:

Side limits: $0.1 < d_3 < 3.0$; $0.1 < d_4 < 3.0$ e $0.1 < r_2 < 3.0$ [u.l.]; (27)
Points above the curve E_1, given by Eq. (6) and Points below the curve E_2, given by Eq. (7).

The ideal solutions calculated using DE were: V_{id}=1896.784 [u.v.]; $Cond(J)_{id}$=1.018 and S_{id}=105.66 [u.s.]. For this case, the optimal results obtained by Weighting Objectives Method are showed in Tab. 3. The Tab. 4 shows the results obtained by using Global Criterion Method. As observed in Example 1, the best solution depends on interest of the designer.

Table 3. Optimal results obtained with the Weighting Objectives Method for Example 2.

weighting coefficients w_i	Technique	d_3 d_4 r_2 (u.l.)	Volume (u.v.)	Cond(J)	Stiffness (u.s)	Time (min)
w_1=0.33	DE	3.00 3.00 3.00	1896.78	1.018	105.66	12.87
w_2=0.33	GA	3.00 3.00 3.00	1896.78	1.018	105.66	55.03
w_3=0.33	SQP	3.00 3.00 3.00	1896.80	1.523	94.00	0.46
w_1=0.80	DE	3.00 3.00 3.00	1896.78	1.018	105.66	66.37
w_2=0.10	GA	3.00 3.00 3.00	1896.78	1.018	105.66	114.02
w_3=0.10	SQP	3.00 3.00 3.00	1896.78	1.018	105.66	0.96
w_1=0.10	DE	3.00 3.00 2.99	1892.50	1.017	105.59	9.80
w_2=0.80	GA	3.00 2.97 2.94	1850.93	1.010	104.12	114.56
w_3=0.10	SQP	3.00 2.97 2.94	1850.96	1.010	104.12	19.08
w_1=0.10	DE	3.00 3.00 3.00	1896.78	1.018	105.66	55.21
w_2=0.10	GA	3.00 3.00 3.00	1896.78	1.018	105.66	119.84
w_3=0.80	SQP	3.00 3.00 3.00	1896.78	1.018	105.66	1.13

Considering the L_{2r}-metric, the optimal point obtained by Differential Evolution is marked in Fig. 6a). The scheme of the optimal manipulator belonging to the topology WT_3 is illustrated in Fig. 6b).

Table 4. Optimal results obtained with the Global Criterion Method for Example 2.

	Technique	d_3 d_4 r_2 (u.l.)	Volume (u.v.)	Cond(J)	Stiffness (u.s)	Time (min)
L_{2r}-metric	DE	3.00 3.00 3.00	1896.78	1.018	105.66	13.35
	GA	3.00 3.00 3.00	1896.78	1.018	105.66	59.78
	SQP	3.00 3.00 3.00	1891.68	1.018	105.56	17.03
L_{3r}-metric	DE	3.00 3.00 3.00	1896.78	1.018	105.66	11.93
	GA	3.00 3.00 3.00	1896.77	1.018	105.66	66.28
	SQP	3.00 3.00 3.99	1888.96	1.016	105.45	14.78

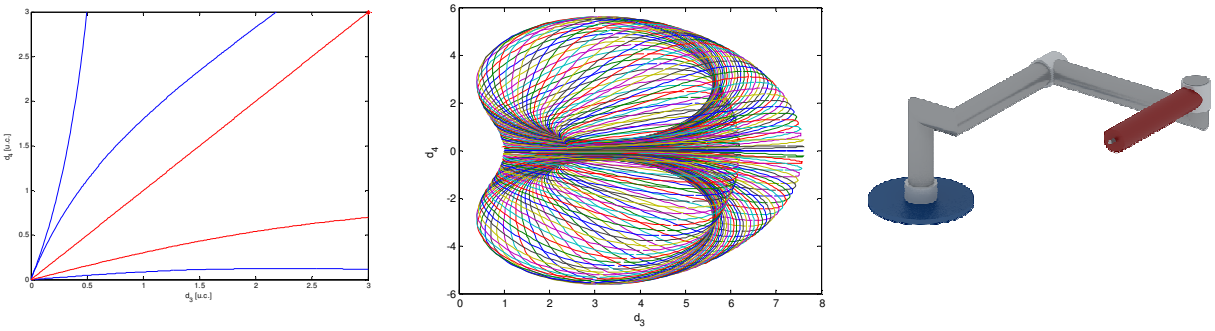

(a)Parameters space with d_2=1, r_3=0 (b) Radial section area of the workspace (c) Scheme for 3R Robot

Figure 6. The optimum design of a 3R Robot, considering the L_{2r}-metric by Differential Evolution – Example 2

The optimal radial section area of the workspace is presented in Fig. 6b). Comparing the radial section of Fig. 6b) to Fig. 3c), one can observe that the workspace is increased. Furthermore, the manipulators of this type of topology remain with 4 cusp points, a region with 4 solutions and other with 2 solutions in IKM.

In Example 1, note that the low values found in relation to ideal values, are due to the difficulties imposed by the constraint C_1. In example 2, the values do not suffer many changes because the restrictions are simpler.

Is important to note that the applied methodologies were effective to obtain optimal solutions obeying the topology constraints.

5.3 Input and Output Window Program

A input data window and a output optimal results window was developed to facilitate the use of computational code, as shown in Fig. 7a) and 7b), respectively.

In the input window the designer can choose the multi-objective optimization method, the type of topology and define the side constraints. In the output window can be seen the volume, stiffness and dexterity optimal values. Moreover, it presents the optimal dimensions and the cross section area of the workspace.

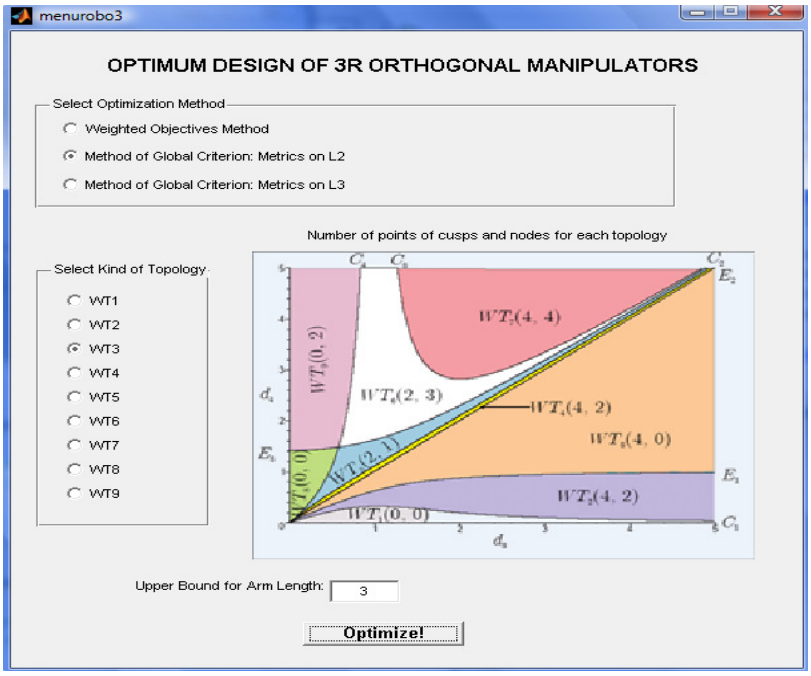

(a)

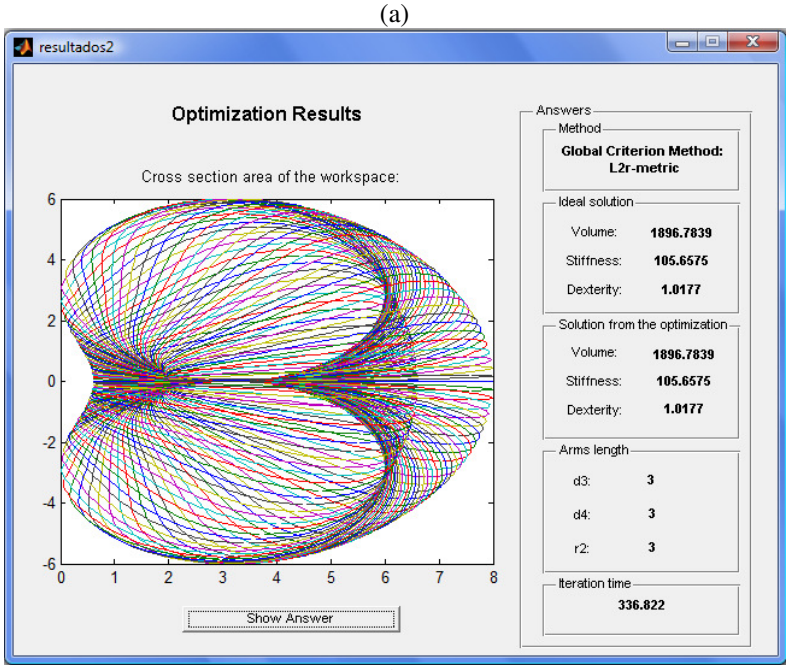

(b)

Figure 7. (a) Input data window; (b) Output optimal results window

6. CONCLUSIONS

In this work, a suitable formulation of the optimal design of manipulators with three orthogonal rotational joints was used. The aim is to obtain the optimal dimensions of the manipulators so that the maximum volume of the workspace, the maximum stiffness of the mechanism and the optimization of dexterity are considered simultaneously.

In addition, were imposed constraints according to the type of workspace topology by using appropriate equations written according to the separation surfaces of the domains. The solutions were obtained by means of two evolutionary techniques and one sequential.

The authors developed a computational code in MATLAB®, easy to be used by the designer, allowing the optimum design of manipulations can be calculated considering the most appropriate topology for the tasks.

The main contributions of this work were: to verify that the dexterity has a great influence on the optimal dimensions of the manipulators; enable the designer to choose one type of topology to obtain the best design that matches the desired application.

In the future work other examples with different topology constraints will be studied and the general case for the 3R manipulator, adopting the parameter $r_3 \neq 0$, will be considered.

7. ACKNOWLEDGEMENTS

The authors acknowledge the Fundação de Amparo a Pesquisa do Estado de Minas Gerais (FAPEMIG) by the financial support.

8. REFERENCES

Baili, M., 2004, “Analise et Classification de Manipulateur 3R à axes Orthogonaux”, Thèse de Doctorat - University of Nantes, France.

Bergamaschi, P.R., Nogueira, A.C. and Saramago, S.F.P., 2006, “Design and optimization of 3R manipulators using the workspace features”, Applied Mathematics and Computation, Elsevier, Vol. 172. No.1., pp. 439-463.

Company, O.,, Pierrot, F., and Fauroux, J. C., 2005, “A method for modeling analytical stiffness of a lower mobility parallel manipulator” Proc. Of IEEE ICRA: Int. Conf. On Robotics and Automation, Barcelona, Spain, April 18-25.

Corvez, S. and Rouillier, F., 2002, “Using computer algebra tools to classify serial manipulators”, Proceeding Fourth International Workshop on Automated Deduction in Geometry, Lins.

Deblaise, D., Hernot, X. and Maurine, P., 2006, “A Systematic Analytical Method for PKM Stiffness Matrix Calculation”, IEEE International Conference on Robotics and Automation.

El-Khasawneh, B. S. andFerreira, P. M., 1999, “Computation of stiffness and stiffness bounds for parallel link manipulator” Int. J. Machine Tools & manufacture, vol. 39(2), pp. 321-342.

Houck, C.R.; Joinez, J.A. and Kay, M.G., 1985, “A Genetic Algorithms for Function Optimization: a Matlab Implementation. NCSO-IE Technical Report”, University of North Caroline, USA.

Gonçalves, R. S., 2009, “Estudo de Rigidez de Cadeias Cinemáticas Fechadas”, Tese de Doutorado - Universidade Federal de Uberlândia, Brasil.

Khalil, W. and Dombre, E., 1999, “Modélisation Identification et Commande des Robots, 2ème édition revue et augmentée”, Hermès, Paris.

Oliveira, G.T.S., Neto, A.D.C., Mendonça, S.A., Saramago, S.F.P., 2008, “Projeto Ótimo de Manipuladores 3R Ortogonais considerando a sua Topologia”, Proceedings of the 5th Congresso nacional de engenharia Mecânica, Associação Brasileira de Mecânica Computacional – ABMEC, Salvador, Brasil.

Oliveira, L.S. and Saramago, S.F.P., 2010, “Multiobjective Optimization Techniques Applied to Engineering Problems”, Journal of the Brazilian Society of Mechanical Sciences and Engineering, Vol.XXXII, pp.94 - 104, 2010.

Nocedal, J., Wright, S.J., 2000, “Numerical Optimization”, Springer Series in Operations Research.

Rivin, E. I., 1999, “Stiffness and Damping in Mechanical Design” Marcel Dekker Inc., New York.

9. RESPONSIBILITY NOTICE

The authors are the only responsible for the printed material included in this paper.